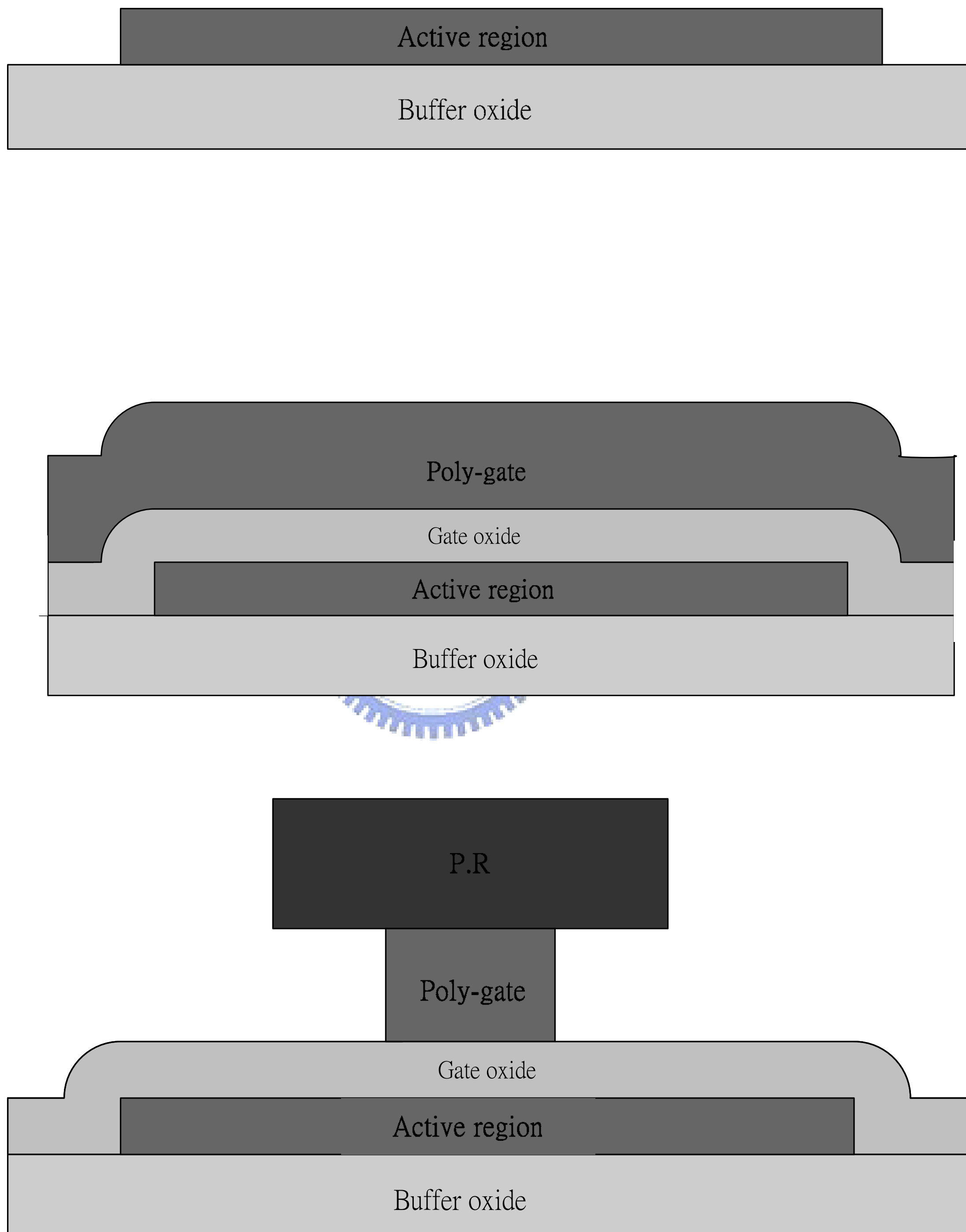

Figure 3.1 Key process flows of T-gate TFTs.

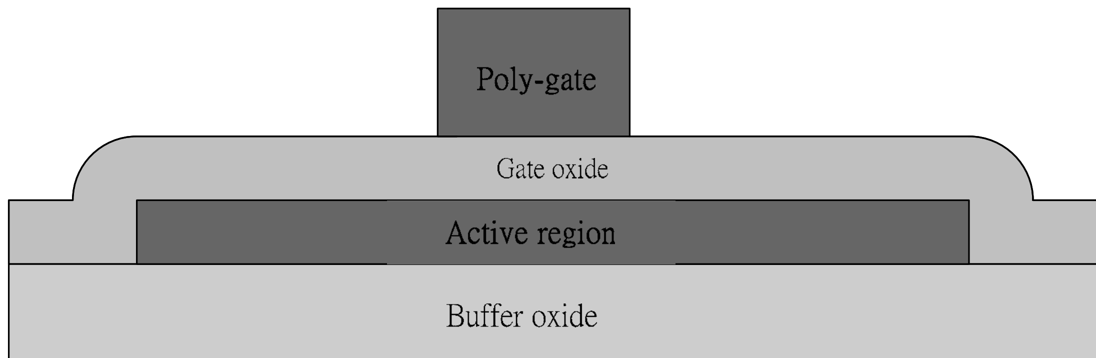

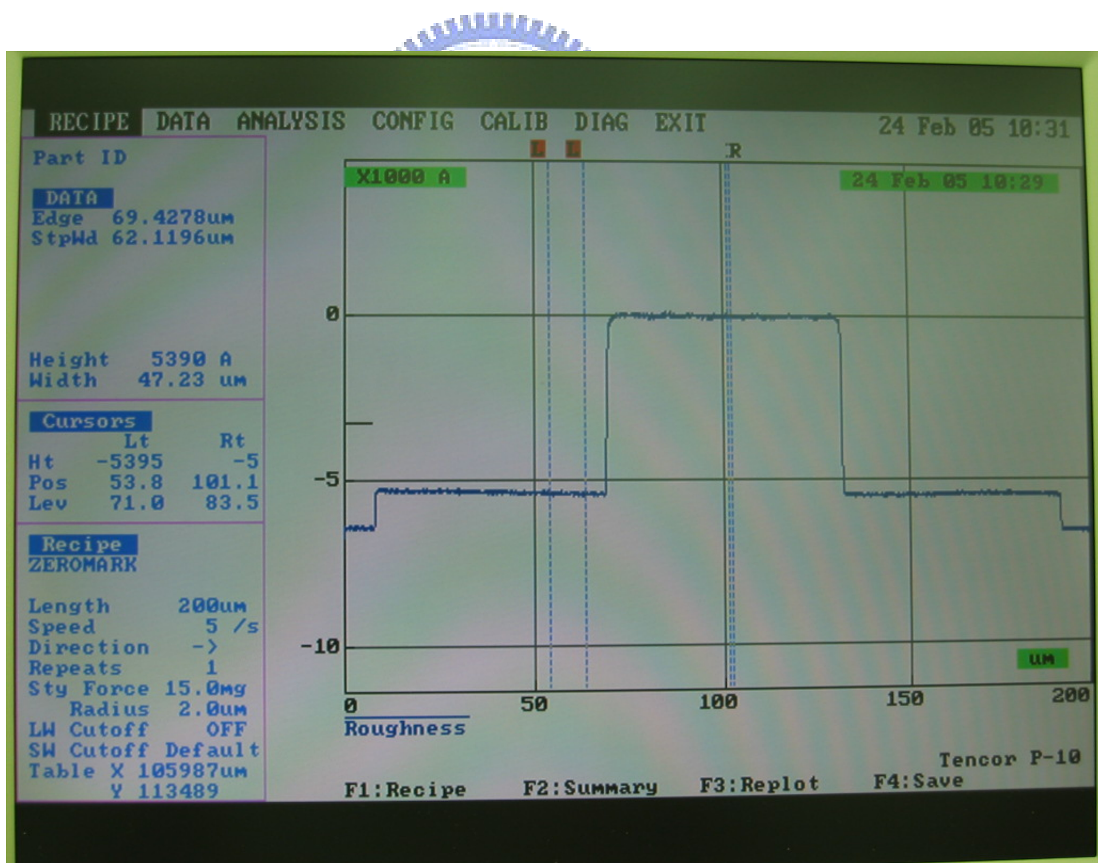

Figure 3.1 Key process flows of T-gate TFTs.

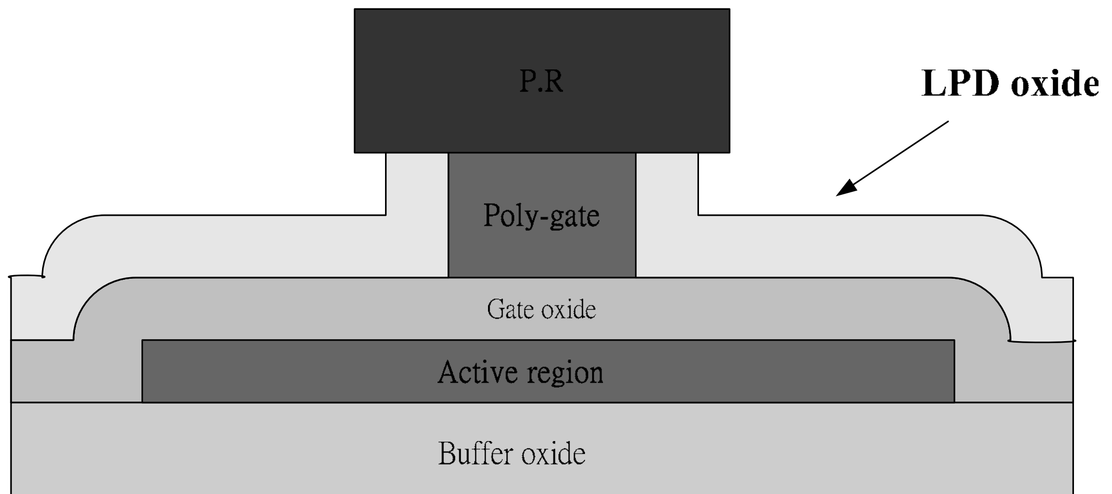
P.R
LPD oxide
Poly-gate
Gate oxide
Active region
Buffer oxide

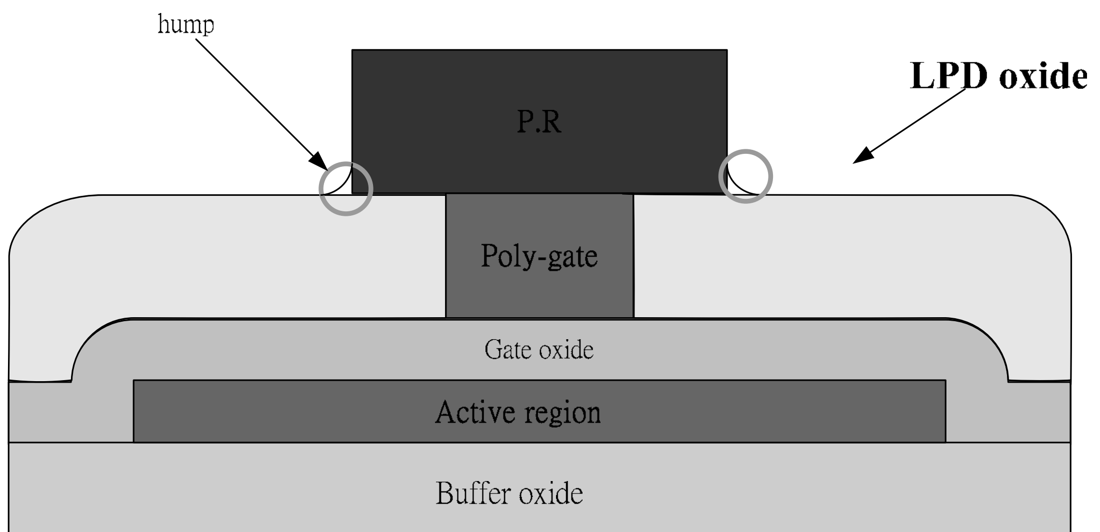
hump
P.R
LPD oxide
Poly-gate
Gate oxide
Active region
Buffer oxide

Figure 3.1 Key process flows of T-gate TFTs.

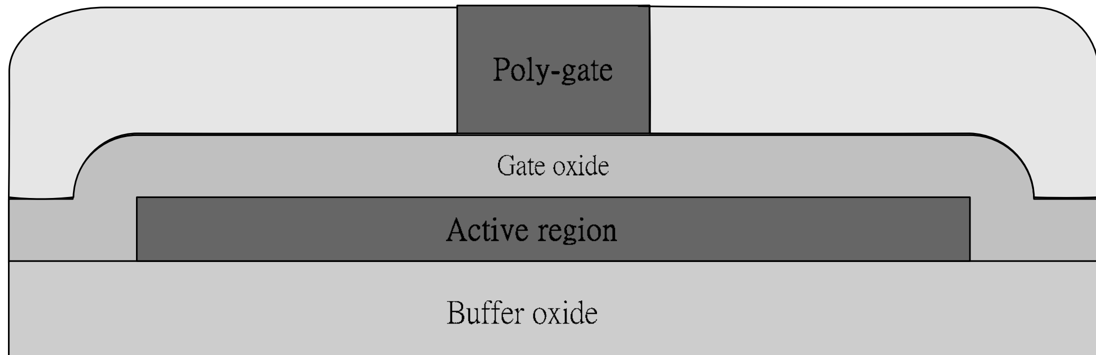

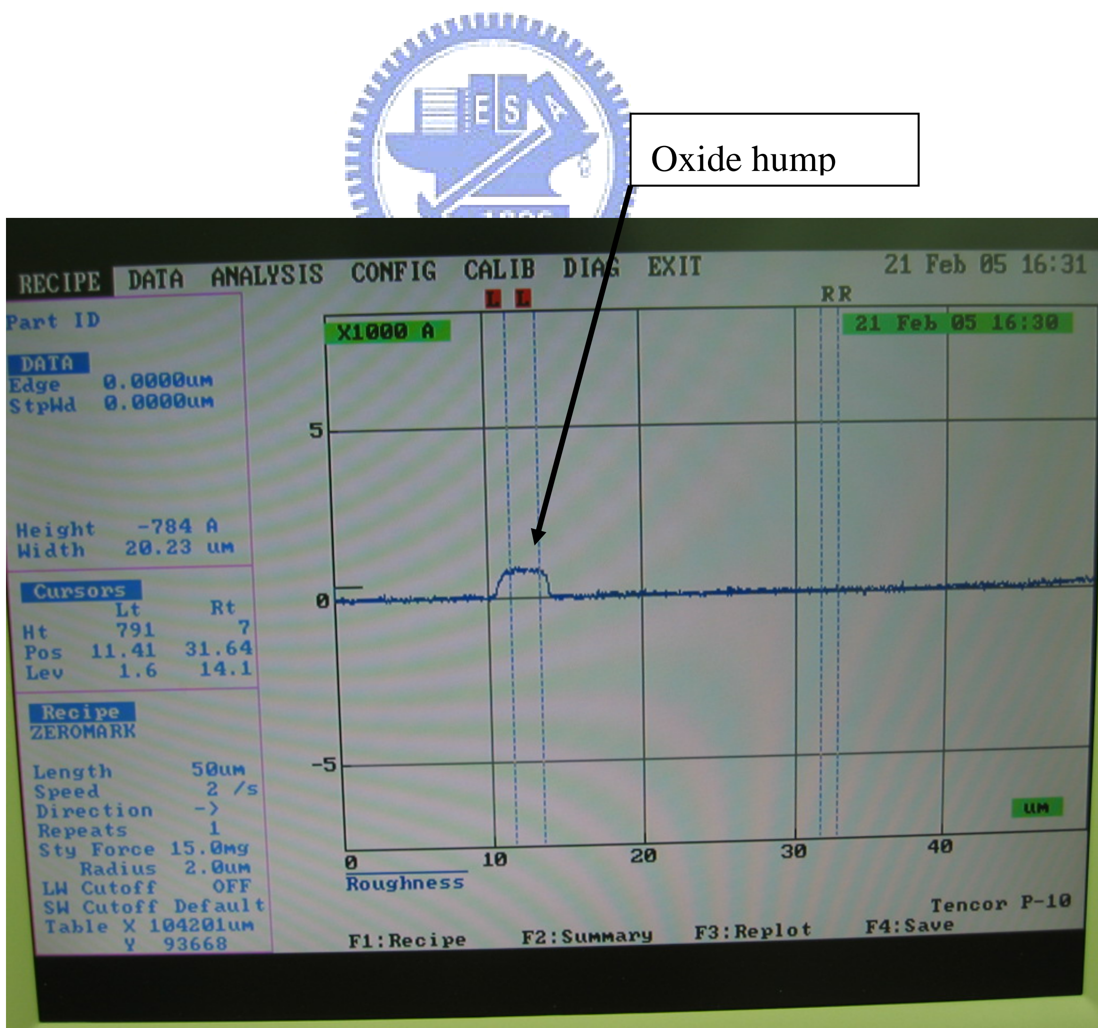

Figure 3.1 Key process flows of T-gate TFTs and surface scan graph.

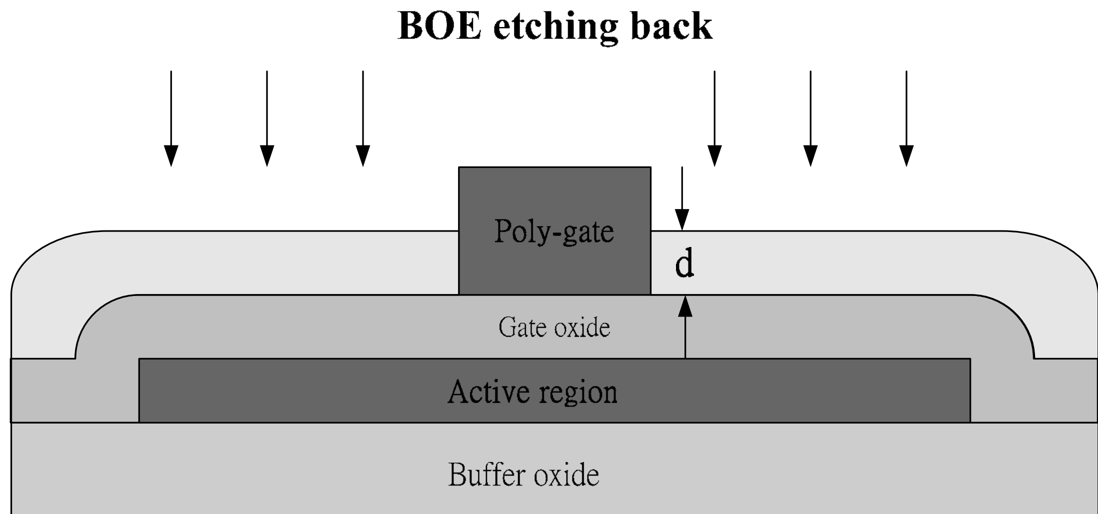

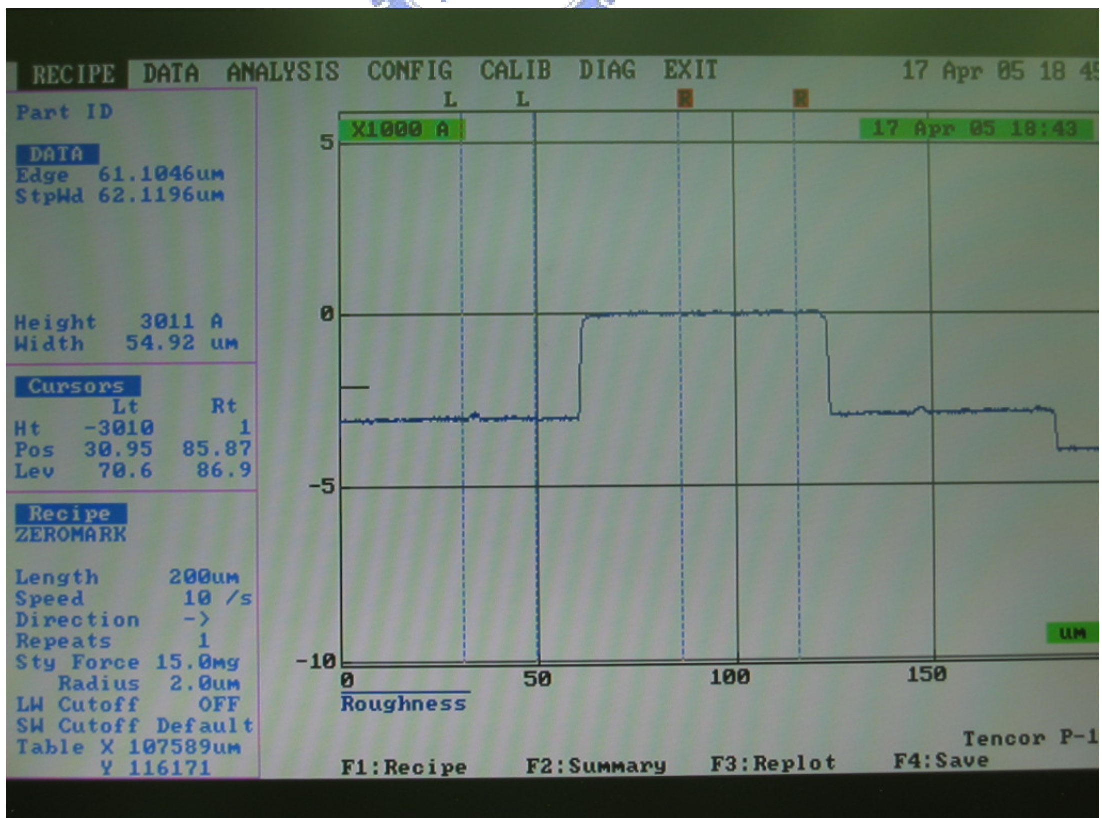

Figure 3.1 Key process flows of T-gate TFTs surface scan graph.

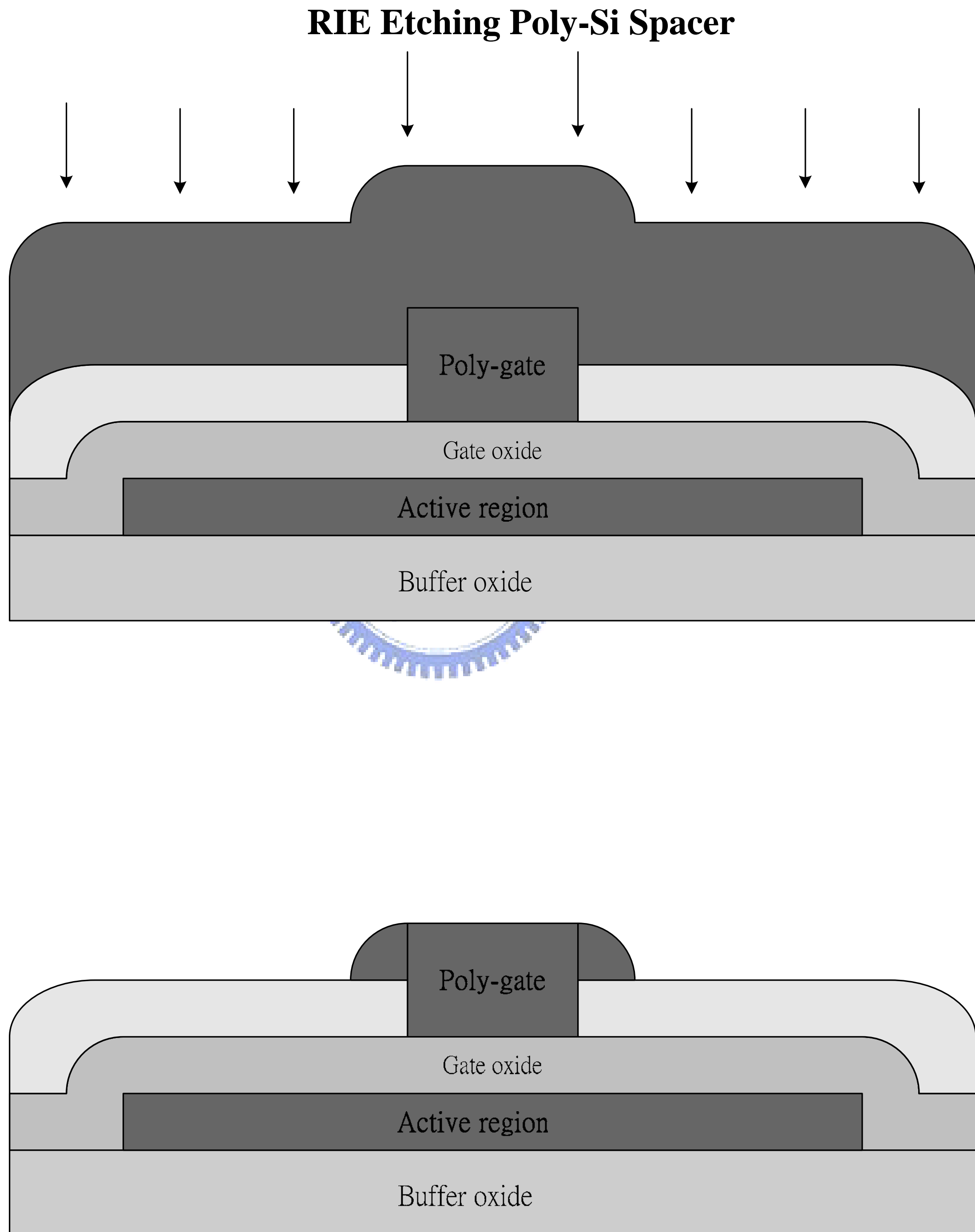

Figure 3.1 Key process flows of T-gate TFTs.

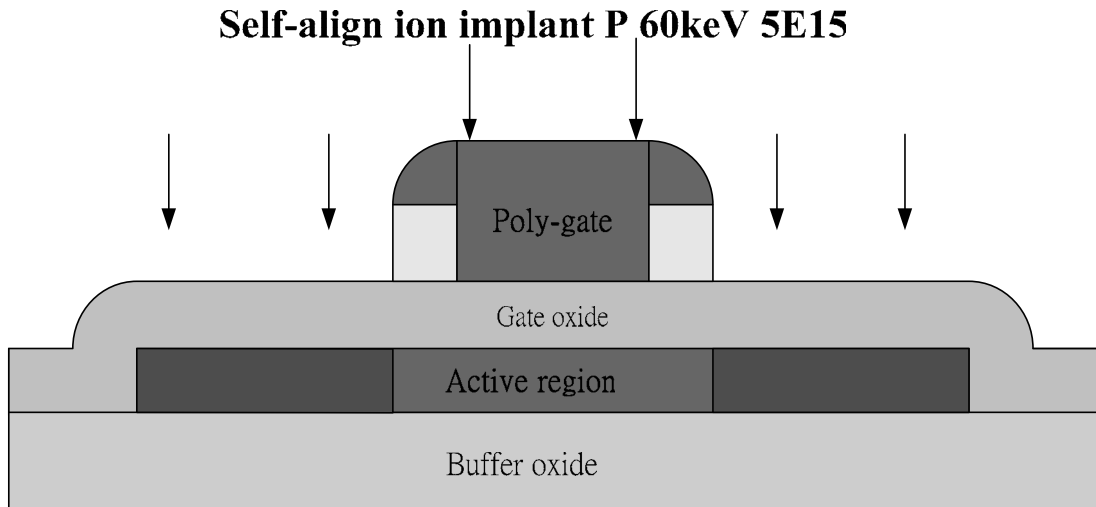

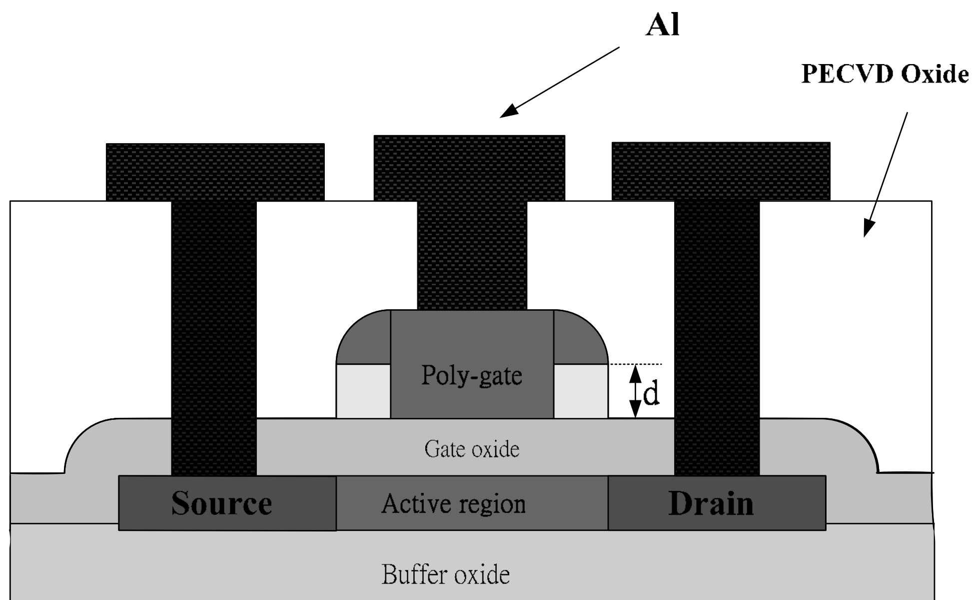

Figure 3.1 Key process flows of T-gate TFTs.

	Vth	mobility	I_{on}	I_{off}	I_{on}/I_{off}
Conventional TFT	**39**	**12.08**	**1.01E-04**	**1.23E-10**	**8.26E+05**
T-gate TFT;d=100nm	**41.1**	**10.54**	**7.10E-05**	**1.06E-10**	**6.67E+05**
T-gate TFT;d=150nm	**42.3**	**9.47**	**6.74E-05**	**9.54E-11**	**7.07E+05**
T-gate TFT;d=200nm	**43.5**	**9.1**	**6.36E-05**	**9.21E-11**	**6.91E+05**

Table 3.1 The electrical characteristics of CTFTs and TGTFTs before plasma treatment.

	Vth	mobility	I_{on}	I_{off}	I_{on}/I_{off}
Conventional TFT	**22.7**	**19.55**	**1.97E-04**	**6.64E-11**	**2.9E+06**
T-gate TFT;d=100nm	**29.4.**	**16.07**	**1.39E-04**	**5.5E-11**	**2.5E+06**
T-gate TFT;d=150nm	**30**	**15.9**	**1.27E-04**	**4.08E-11**	**3.1E+06**
T-gate TFT;d=200nm	**30.6**	**15.22**	**1.18E-04**	**6.18E-11**	**1.9E+06**

Table 3.2 The electrical characteristics of CTFTs and TGTFTs after plasma treatment.

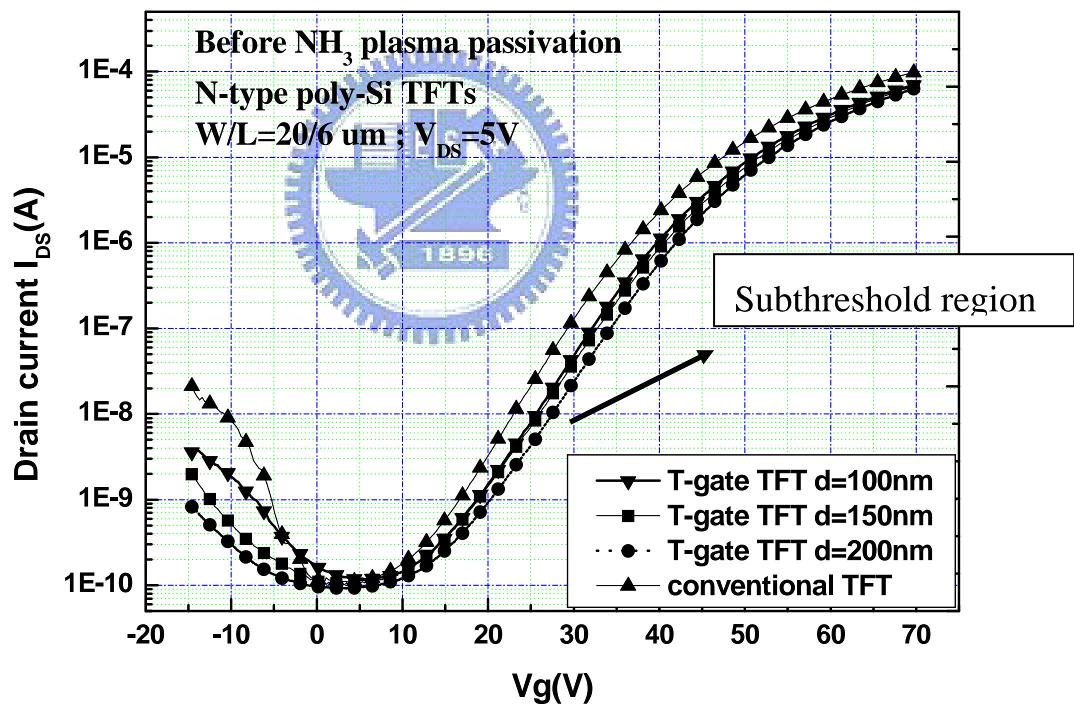

Figure 3.2 (a) Transfer characteristics for comparison of CTFT and TGTFT with difference offset oxide thickness before plasma treatment.

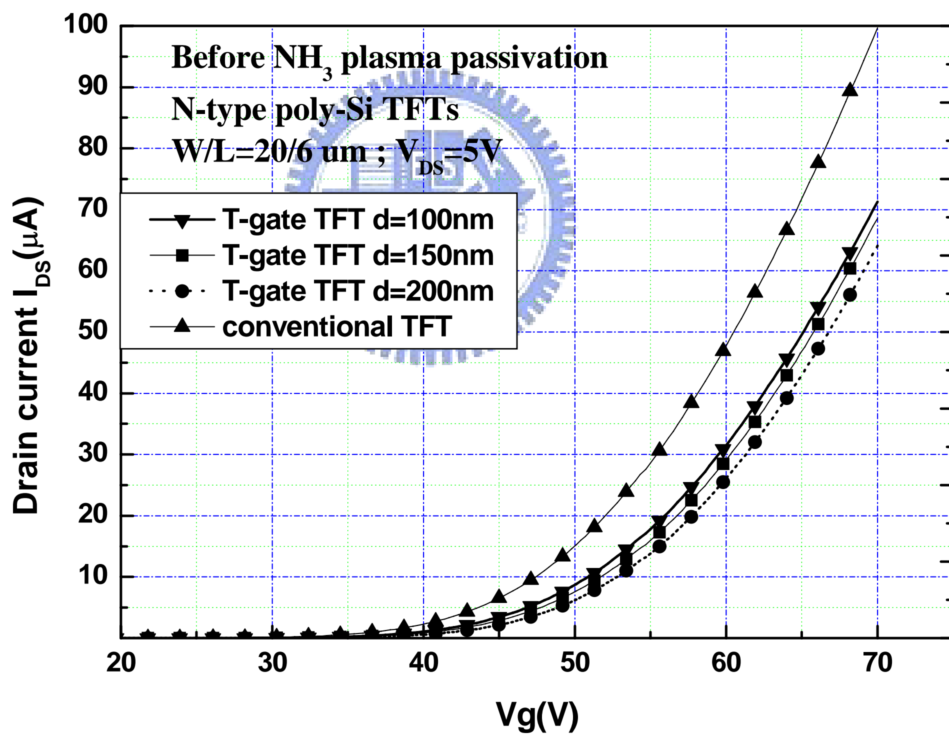

Figure 3.2 (b) Transfer characteristics (linear scale) for comparison of CTFT and TGTFT with difference offset oxide thickness before plasma treatment.

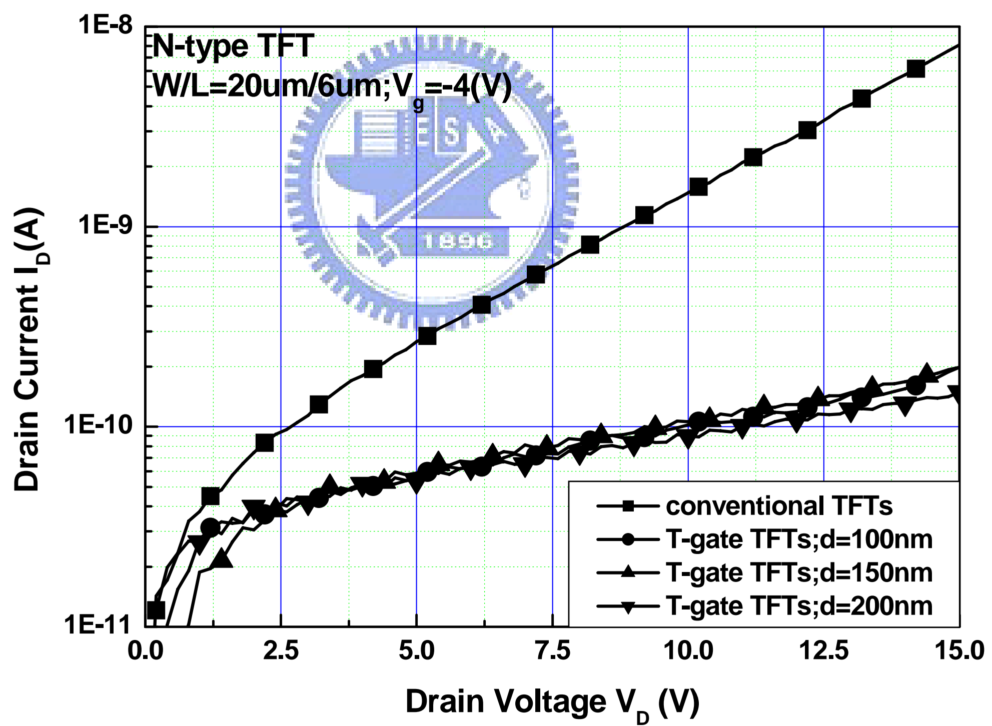

Figure 3.3 Leakage current, measured at Vg = - 4 V, for CTFT and TGTFT with W/L = 20/6 and different offset oxide thickness.

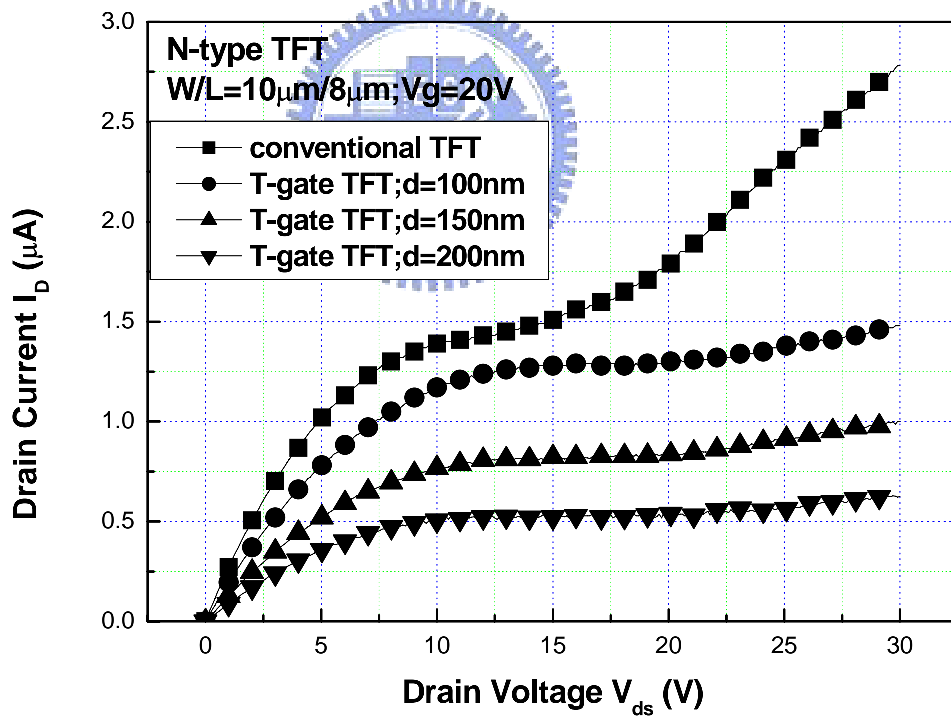

Figure 3.4 The Id – V_D characteristics curve for CTFT and TGTFT with W/L = 10/8 measured at Vg = 20 V.

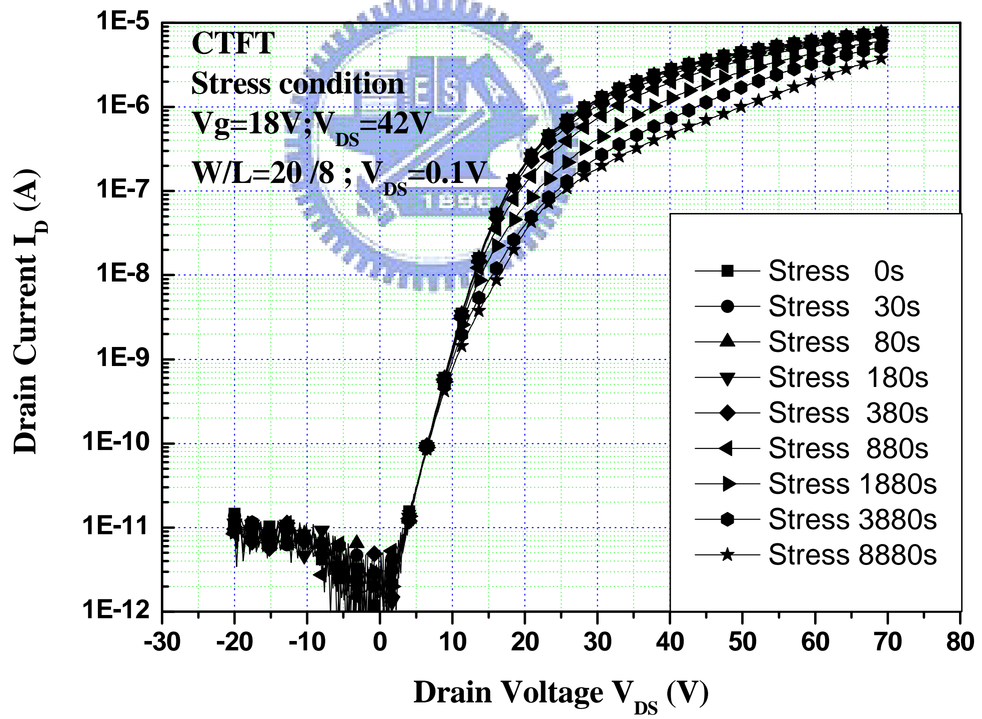

Figure 3.5 (a) The Id – V_D characteristics curve for CTFT before and after the application of hot- carrier stress (W/L = 10/8 measured at Vg = 20 V).

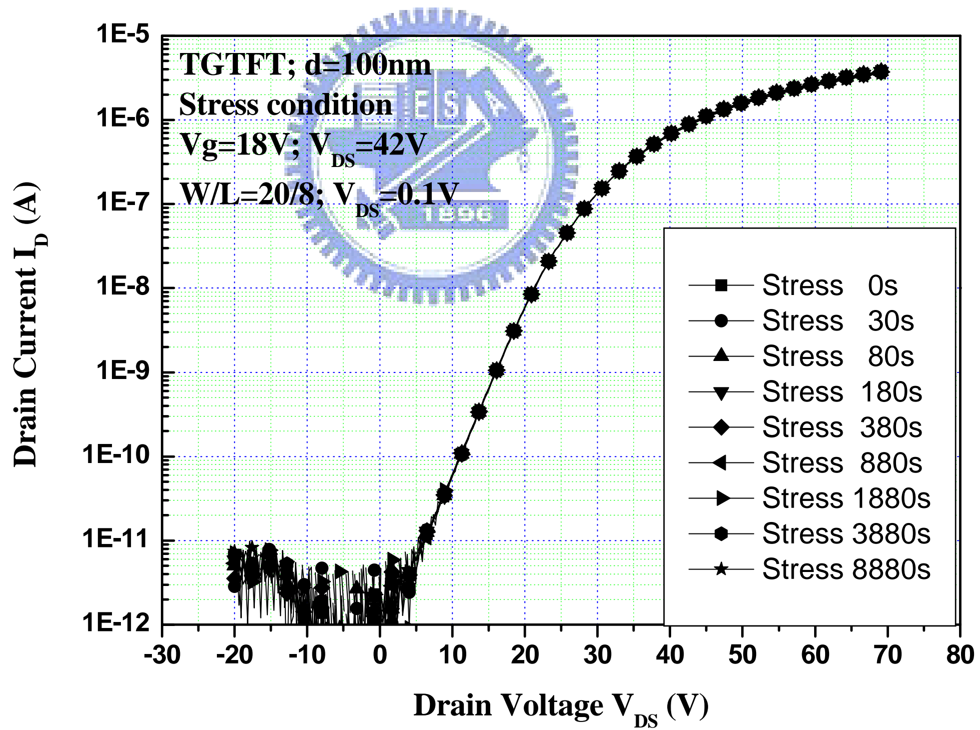

Figure 3.5 (a) The Id – V_D characteristics curve for TGTFT before and after the application of hot- carrier stress (W/L = 10/8 measured at V_{DS} = 0.1V).

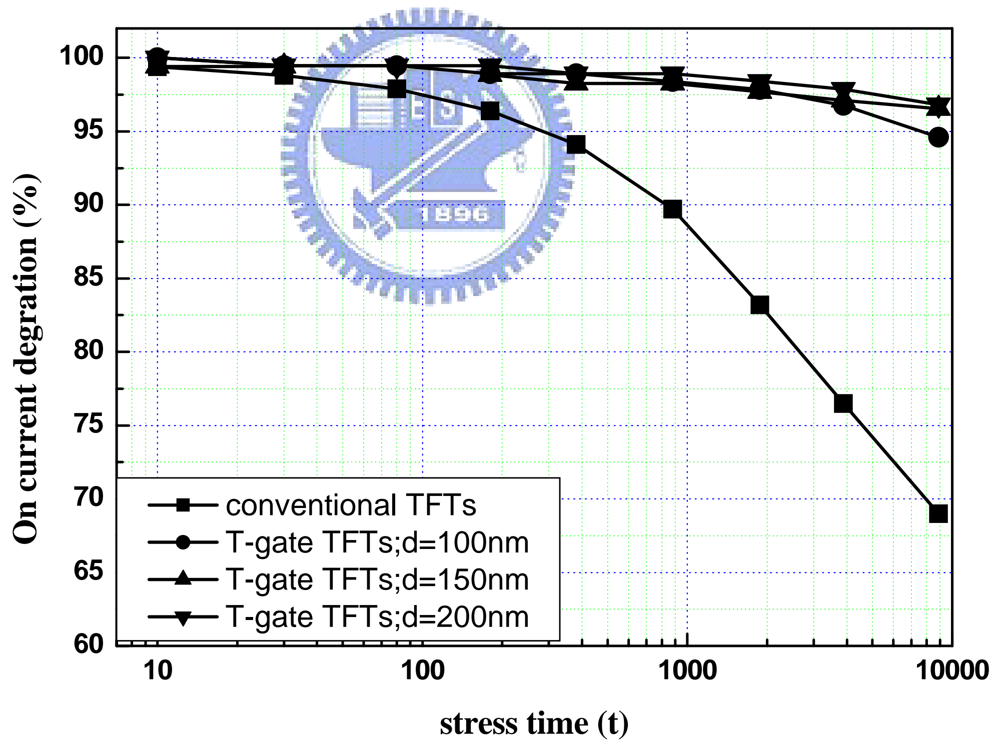

Figure 3.6 (a) Comparison of degradation rate of ON-state current after hot carrier stress (stress condition: V_g= 18 V, V_{DS}= 42 V) with W/L = 10/8.

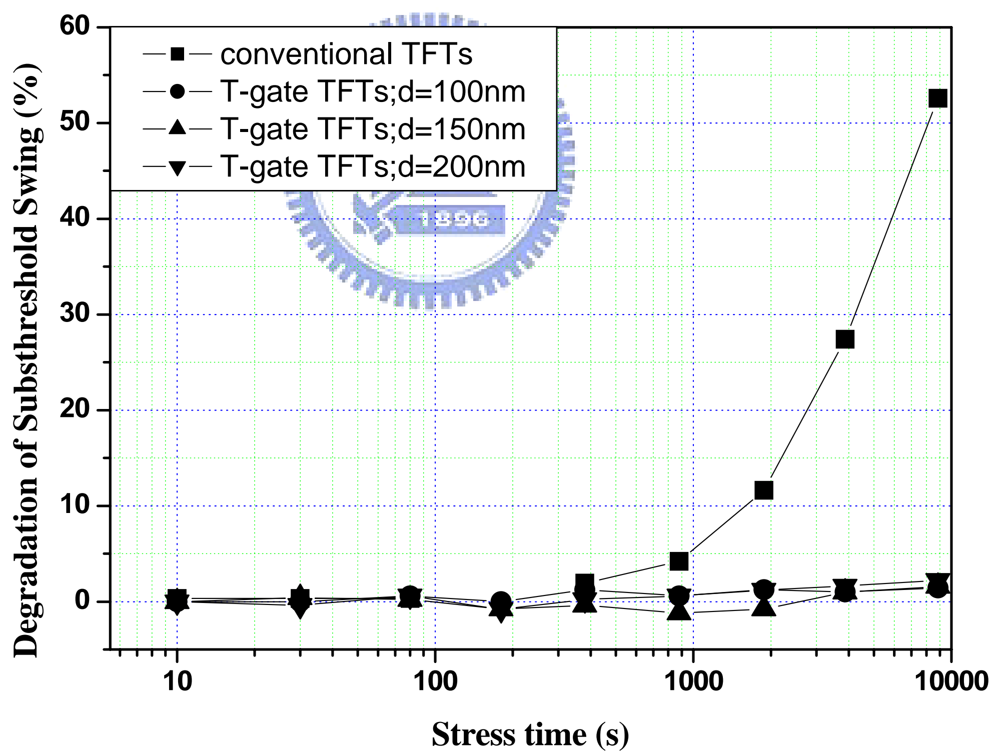

Figure 3.6 (b) Comparison of degradation rate of subtrhreshold swing after hot carrier stress (stress condition: V_g= 18 V, V_{DS}= 42 V) with W/L = 10/8.

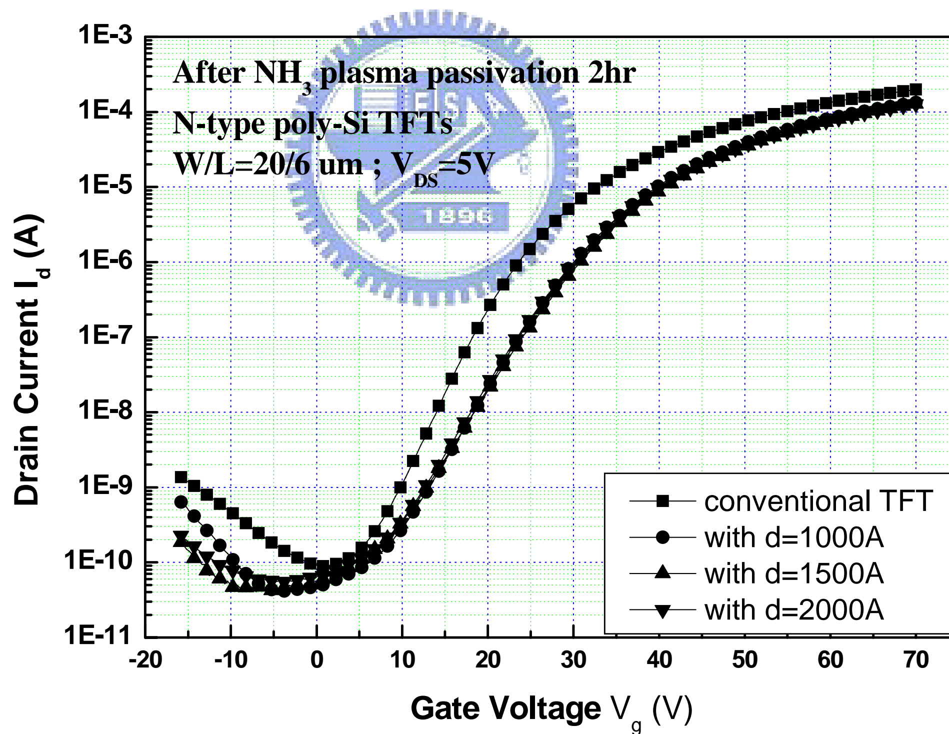

Figure 3.7 Transfer characteristics for comparison of CTFT and TGTFT with difference offset oxide thickness after plasma treatment 2hr.

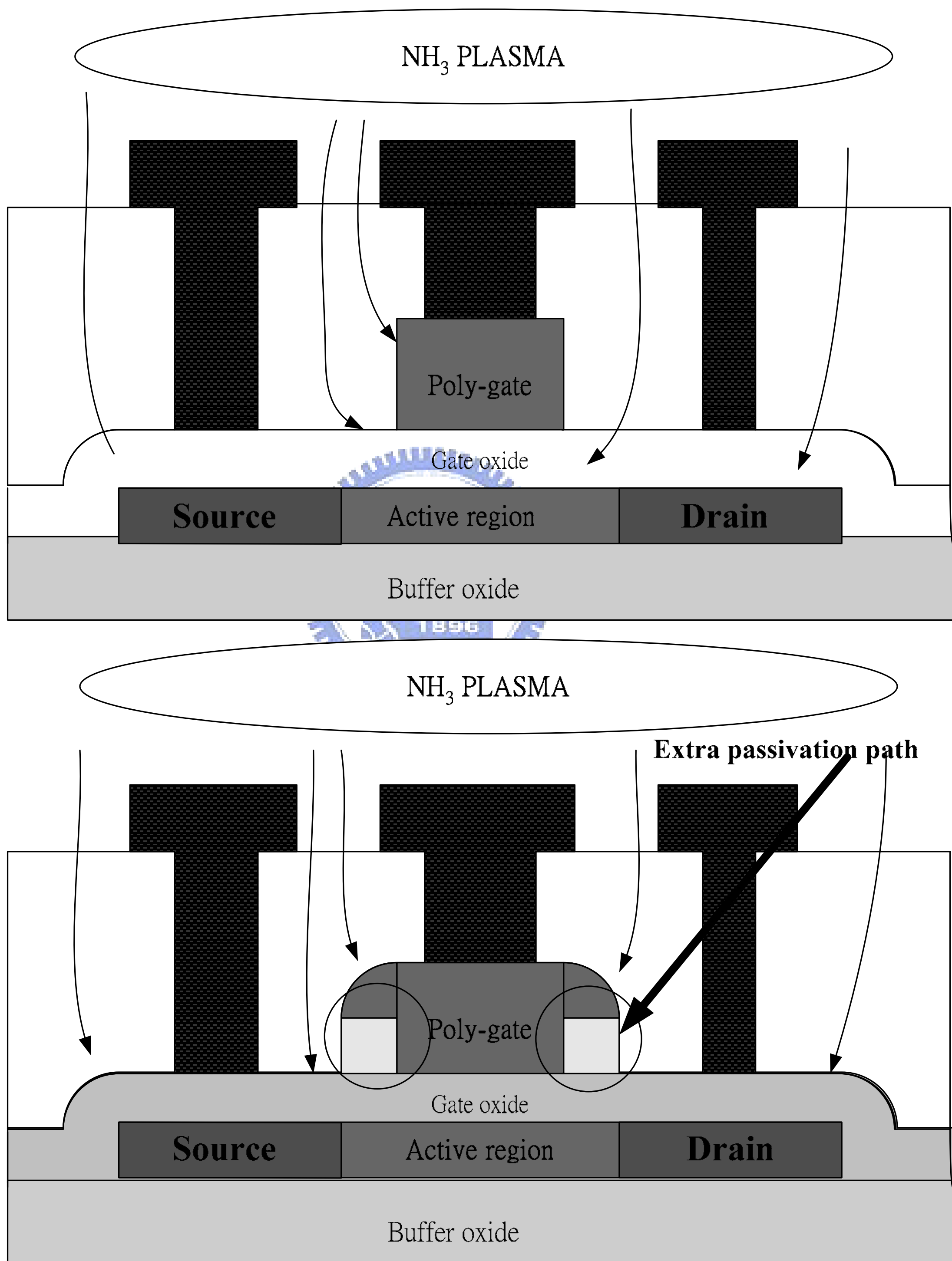

Figure 3.8 The pathway for hydrogen migration from a gaseous source to the active channel region of (a) conventional TFTs and (b) TGTFTs.

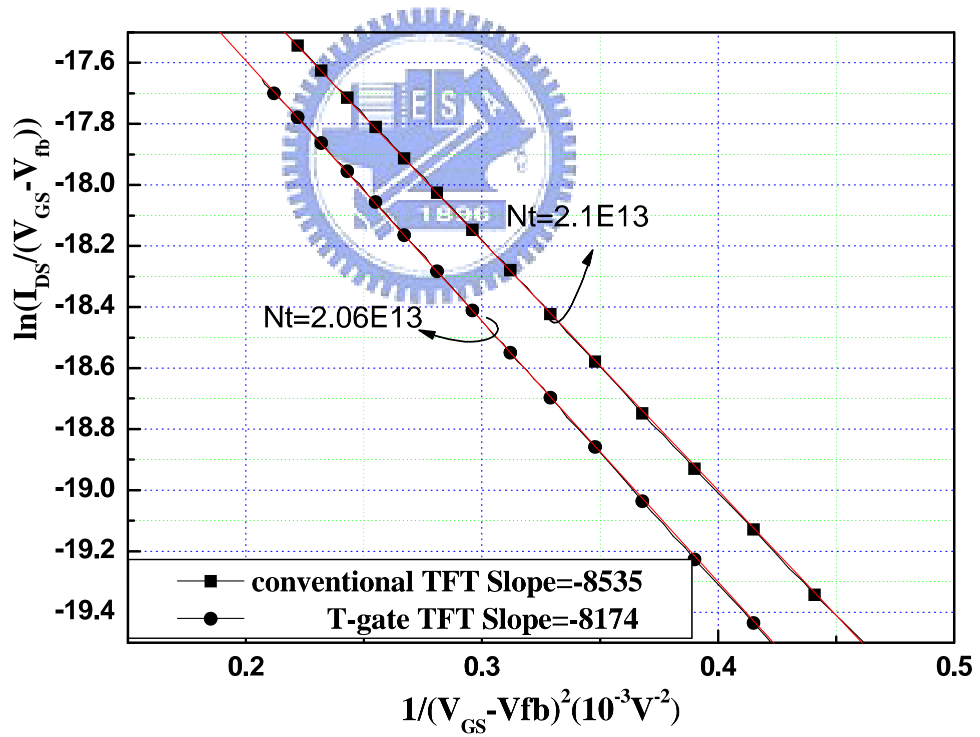

Figure 3.9 (a) Extraction of trap-state density (Nt) by the modified Levinson theorem for CTFT and TGTFT before plasma treatment.

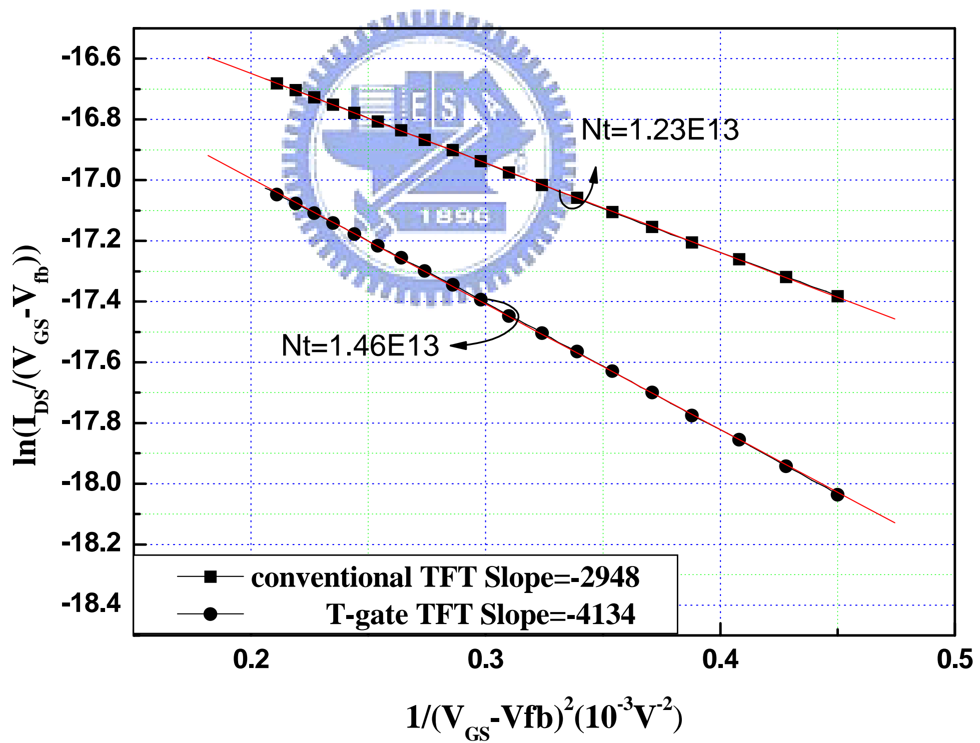

Figure 3.9 (b) Extraction of trap-state density (Nt) by the modified Levinson theorem for CTFT and TGTFT after plasma treatment 2hr.

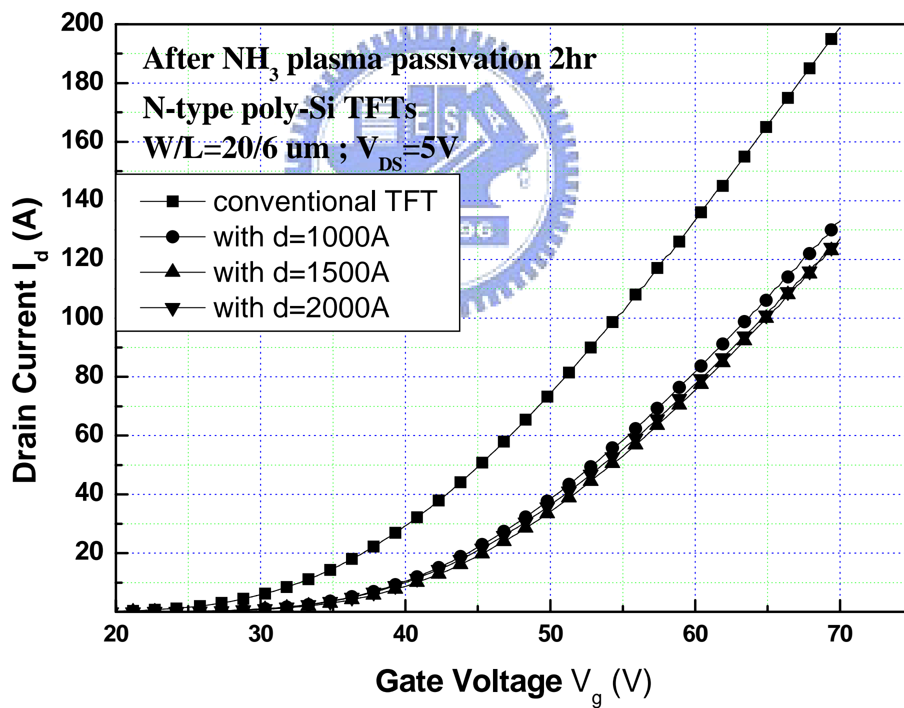

Figure 3.10 Transfer characteristics (with linear scale) for comparison of CTFT and TGTFT with difference offset oxide thickness after plasma treatment 2hr